THE JOURNAL OF PHYSICAL CHEMISTRY C

ARTICLE

pubs.acs.org/JPCC

# Solution-Phase Desorption of Self-Assembled Monolayers on Gold Derived From Terminally Perfluorinated Alkanethiols

Yuehua Yuan,[†] Chi Ming Yam,[†] Olga E. Shmakova,[†] Ramon Colorado, Jr.,[†] Michael Graupe,[†] Hitoshi Fukushima,[‡] H. Justin Moore,[*,§] and T. Randall Lee[*,†]

[†]Department of Chemistry and the Texas Center for Superconductivity, University of Houston, Houston, Texas 77204-5003, United States

[‡]Core Technology Development Centre, Seiko Epson Corporation, 281 Fujimi, Fujimi-machi, Suwa-gun, Nagano-ken 339-0293, Japan

[§]Department of Chemistry and Environmental Sciences, University of Texas at Brownsville, Brownsville, Texas 78520, United States

**ABSTRACT:** The solution-phase thermal desorption of three series of self-assembled monolayers (SAMs) on gold generated from terminally perfluorinated alkanethiols was examined. Series 1 SAMs, $F(CF_2)_x(CH_2)_{11}SH$, where $x = 1-10$, consisted of a constant hydrocarbon segment length with an increasing fluorocarbon segment length. Series 2 SAMs, $F(CF_2)_{10}(CH_2)_y$-SH, where $y = 2-6$, 11, consisted of a constant fluorocarbon segment length with an increasing hydrocarbon segment length. Series 3 SAMs, $F(CF_2)_x(CH_2)_ySH$, where $x = 1-10$ and $y = 16 - x$, consisted of both hydrocarbon and fluorocarbon segments in which the segment lengths were varied while holding the total chain length constant at 16 carbon atoms. SAMs from these three series were prepared and characterized using both ellipsometry and contact-angle measurements. The resultant SAMs were shown to be highly hydrophobic and oleophobic. The SAMs were heated in decalin (DC) and perfluorodecalin (PFD) at 80 °C for various periods of time to monitor their thermal stability when exposed to hydrocarbon versus fluorocarbon solvents. In general, SAMs derived from *n*-alkanethiols and terminally perfluorinated alkanethiols exhibited diminished thermal stabilities upon heating in a hydrocarbon solvent (DC) versus heating in a perfluorocarbon solvent (PFD). The thermal stability of the SAMs increased with increasing lengths of the $CF_2$ or $CH_2$ segments. We also examined the kinetics of thermal desorption of these SAMs. From these studies, SAMs composed of higher degrees of terminal perfluorination exhibited smaller rate constants for the initial stage (fast regime) of desorption. When compared with analogous alkanethiol SAMs, the terminally perfluorinated SAMs exhibited greater thermal stabilities in both DC and PFD. In addition, values of the rate constants for desorption of the alkanethiol SAMs were approximately double those of the terminally perfluorinated SAMs having similar chain lengths.

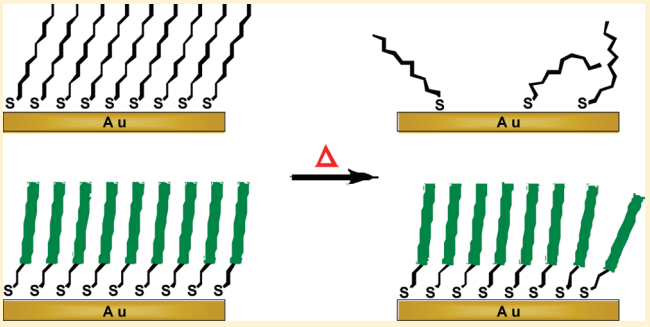


## INTRODUCTION

The study of metal−supported self-assembled monolayers (SAMs) first emerged in 1946 when Zisman published his work on surfactants that self-assemble onto clean metal substrates.[1] The potential for using the specific interaction between sulfur and gold was realized by Taniguchi et al.[2] in their electrochemical studies of bis(4-pyridyl) disulfide-modified electrodes in 1982. Intense interest in this field grew rapidly following the 1983 studies by Nuzzo and Allara, who reported the spontaneous formation of SAMs upon exposure of gold substrates to dilute solutions of di-*n*-alkyl disulfides.[3] SAMs on gold derived from di-*n*-alkyl disulfides and analogous alkanethiols are attractive nanoscale tools because they offer the ability to control interfacial properties through simple chemical synthesis. Consequently, SAMs are now used in a variety of applications, including microelectronics;[4−6] bioadhesion-resistant surfaces;[7−11] biosensors;[12−14] photochemistry;[15,16] and perhaps most importantly, corrosion prevention.[17−23]

Although SAMs have shown great potential in countless areas of research, an evaluation of their stabilities in solution and at elevated temperatures remains incomplete. It is known that SAMs on gold derived from normal long-chain alkanethiols form highly ordered, well-packed films because of van der Waals interactions between neighboring chains.[24,25] Nevertheless, these SAMs exhibit only moderate thermal stability under ambient conditions[26−28] and typically decompose upon heating at temperatures above 80 °C in solution.[25,29] Additional factors that limit the durability of alkanethiol-based SAMs on gold include their facile oxidation by atmospheric levels of ozone,[30−33] their displacement from the surface by immersion in a solution containing a different adsorbate molecule,[34−36] and their ability to migrate on the gold surface.[37,38] Considering these issues, efforts to enhance the durability of the films have employed strategies such as the utilization of intermolecular hydrogen bonding,[39−42] multiple headgroup-substrate interactions,[43−53] cross-linking between neighboring adsorbates,[54] underpotential

**Received:** May 28, 2011
**Revised:** August 19, 2011
**Published:** August 29, 2011

ACS Publications © 2011 American Chemical Society



dx.doi.org/10.1021/jp204970b | *J. Phys. Chem. C* 2011, 115, 19749–19760

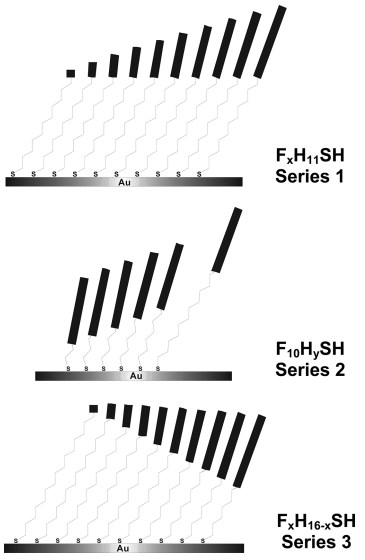


**Figure 1.** SAMs on gold derived from the adsorption of three classes of terminally perfluorinated alkanethiols.

metal deposition,[22,55−57] and the replacement of hydrocarbons with fluorocarbons.[58]

Related studies have examined the stability of alkanethiolate SAMs under various conditions, including ultrahigh vacuum (UHV),[59,60] ambient laboratory conditions,[26] and contact with hydrocarbon solvents.[52] Most of these studies and those in the preceding paragraph agree that a major pathway for the decomposition of alkanethiolate-based SAMs on gold involves the oxidation of the thiolate-gold bond by atmospheric ozone,[30,31] diffusing to the substrate surface through defects in the monolayer. Consequently, the generation of SAMs having densely packed long-chain adsorbates restricts the diffusion of ozone and affords SAMs with enhanced stabilities.

Because of their intriguing inertness, stability, and potential use as nanoscale corrosion inhibitors, interest in the study of SAMs generated from the adsorption of partially fluorinated alkanethiols or alkyldisulfides onto the surface of gold has garnered substantial interest.[38,58,61−70] These studies have found that monolayer films derived from fluorinated alkanethiols are generally robust and essentially defect-free, with the perfluorocarbon segment adopting a helical conformation and possessing a larger van der Waals diameter (∼5.8 Å) than those of trans-extended hydrocarbon chains (∼4.2 Å).[61,62,68] As a result, the perfluorocarbon helix augments the film rigidity compared with corresponding hydrocarbon chains,[65] further enhancing their inertness[67] and thereby contributing to their resistance to oxidation[71] and degradation.[72−74]

In a previous study, we evaluated the relationship between film stability and the length of the underlying methylene spacer in a series of perfluorodecyl-terminated SAMs on gold.[58] Specifically, SAMs generated from a series of terminally perfluorinated alkanethiols ($F(CF_2)_{10}(CH_2)_ySH$, where $y$ = 2, 6, 11, 17, 33), which possessed a constant degree of perfluorination but a variable length of methylene spacer, were incubated in air at various temperatures up to 180 °C. These studies concluded that film durability increased systematically with increasing length of the methylene spacer, which was attributed to increased van der Waals interactions between neighboring methylene chains.

In the present study, we explored the thermal stability of three series of terminally perfluorinated SAMs on gold (Figure 1), in which the substrates were immersed in organic solvents at elevated temperature (80 °C): $F(CF_2)_x(CH_2)_{11}SH$, where $x$ = 1−10 (Series 1); $F(CF_2)_{10}(CH_2)_ySH$, where $y$ = 2−6, 11 (Series 2); and $(F(CF_2)_x(CH_2)_ySH$, where $x$ = 1−10 and $y = 16 - x$ (Series 3). Fresh SAMs were placed in a high-boiling branched hydrocarbon solvent (decalin; DC) and separately in its bulkier perfluorinated analogue (perfluorodecalin; PFD) heated at 80 °C. We monitored the stability of the resulting films through contact-angle and ellipsometry measurements under controlled conditions. By systematically varying the type of solvent (hydrocarbon vs fluorocarbon) and the relative lengths of the hydrocarbon and fluorocarbon segments in the SAMs, these studies were designed to reveal the important considerations necessary for the design of highly stable nanoscale surface coatings.

## EXPERIMENTAL SECTION

**Materials.** Gold shot (99.999%) was purchased from Americana Precious Metals, and chromium rods (99.9%) were purchased from R. D. Mathis Co. Single-crystal silicon (100) wafers were purchased from Silicon Sense, Inc. and were rinsed with absolute ethanol prior to use. The various *n*-alkanethiols, $H(CH_2)_xSH$ ($x$ = 10, 12, 14, 16, 18, 20) were purchased from Aldrich and used without purification. The solvents decalin (DC), perfluorodecalin (PFD), absolute ethanol, and hexadecane (HD) were of the highest purity available purchased from commercial suppliers. The terminally perfluorinated alkanethiols used in this study were either available from previous studies or were prepared using procedures described therein.[64,69,75]

**Preparation of Substrates.** Gold substrates were prepared by thermal evaporation under vacuum ($1 \times 10^{-5}$ Torr) of a 100 Å adhesion layer of chromium onto the surface of polished silicon wafers, followed by the evaporation of 2000 Å of gold. The gold-coated wafers were cut with a diamond-tipped stylus (∼1 × 3 cm), rinsed with absolute ethanol, and dried with a stream of ultrapure nitrogen before collecting base ellipsometric constants and then further use.

**Preparation of SAMs.** All glassware was previously cleaned with piranha solution (7:3 $H_2SO_4/H_2O_2$). *Caution: Piranha solution reacts violently with organic materials and should be handled carefully!* The clean, gold-coated wafers were incubated in a 1 mM ethanolic solution of the respective thiol for at least 24 h, followed by rinsing with absolute ethanol and drying with ultrapure nitrogen.

**Contact Angle Goniometry.** The contacting liquids (water, HD, and PFD) were dispensed onto the surface of the monolayers using a Matrix Technologies micro-Electrapette 25. Advancing contact angles were measured with a Ramé-Hart model 100 contact angle goniometer with the pipet tip in contact with the drop. Reported values for each SAM are the average of measurements recorded from at least two different slides and measuring three drops per slide. Measured contact angles were reproducible to within ±2° of the values reported. All contact angle measurements were conducted at room temperature with the pipet tip in contact with the drop.

**Ellipsometric Thickness.** The thicknesses of the SAMs were measured with a Rudolph Research Auto EL III ellipsometer equipped with a 632.8 nm He−Ne laser at an incident angle of 70°. A refractive index of 1.45 was assumed for all SAMs.[25,76] The reported values were reproducible to within ±2 Å and were the average of at least six measurements taken at different locations on at least two different samples.

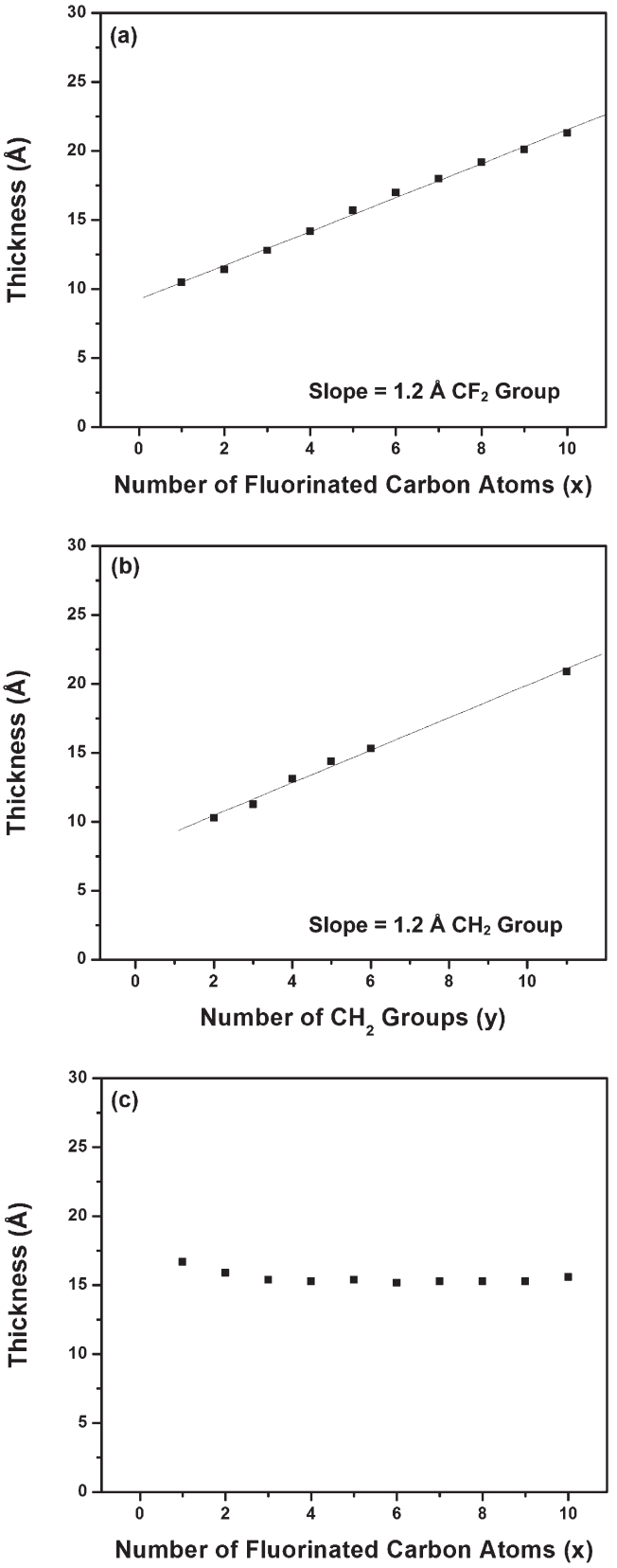


**Figure 2.** Ellipsometric thicknesses of SAMs on gold generated from (a) Series 1, (b) Series 2, and (c) Series 3.

**Evaluation of Thermal Stability.** The perfluorinated alkanethiol and *n*-alkanethiol SAMS were heated in unstirred solutions of either DC or PFD (5 mL) at 80 °C as a function of time, followed by rinsing with absolute ethanol and drying with ultrapure nitrogen. The samples were then immediately subjected to analysis by ellipsometry and then contact angle goniometry. Using a previously developed analytical method,[25,55] relative ellipsometric thicknesses were used to determine the fraction of SAM remaining on the surface. Further, given that contact angle measurements can be sensitive to the orientation, composition, and conformational order of organic thin films,[77] we collected advancing contact angle data before and after the SAMs were subjected to thermal treatment in each solvent. In particular, contact angles of hexadecane (HD) are particularly useful in monitoring subtle changes in the structure or orientation of low energy surfaces.[78,79]

## RESULTS AND DISCUSSION

**A. Characterization of Freshly Prepared SAMs.** *Ellipsometric Characterization. Series 1, $F(CF_2)_x(CH_2)_{11}SH$.* We utilized ellipsometry to determine the initial thicknesses of the SAMs from Series 1 and to evaluate the bulk changes in film thickness as a function of thermal treatment. Figure 2a shows the ellipsometric thicknesses of Series 1 SAMs, which are consistent with those previously reported,[80] indicating that these SAMs correspond to uniform, densely packed monolayer films. The thicknesses increase linearly with an increase in the number of $CF_2$ units ($x$). The slope in Figure 2a was calculated from the least-squares linear regression line through the data points and corresponds to the film thickness per $CF_2$ unit (i.e., 1.2 Å per $CF_2$), which is in good agreement with a previous report.[80] Although ellipsometry cannot directly detect the existence of surface defects that can plausibly influence the desorption of SAMs, both AFM images[67] and resistance measurements[70] of SAMs on gold derived from several terminally fluorinated thiols (including several of the adsorbates examined here) suggest that the fluorinated SAMs possess no more defects than SAMs derived for *n*-alkanethiols. Consequently, we can reasonably assume that SAMs generated from Series 1, 2, and 3 adsorbates all demonstrate similarly low defect densities.

*Series 2, $F(CF_2)_{10}(CH_2)_ySH$.* In Figure 2b, the ellipsometric thicknesses of Series 2 SAMs show a linear relationship between film thickness and an increase in the number of $CH_2$ units ($y$) in the hydrocarbon segment. The linear regression line through the data points gives a slope of 1.2 Å per $CH_2$ unit, which also agrees with the previous study.[80] In contrast, we note that ellipsometric thickness measurements of *n*-alkanethiolate SAMs on gold have found a slope of 1.5 Å per $CH_2$ unit.[24,25] Given that a separate study determined that the $CH_2$ moieties of semifluorinated SAMs are tilted more from the surface normal than those of *n*-alkanethiol SAMs,[69] the smaller slope observed here is likely due to the greater tilt of the hydrocarbon segments in the Series 2 SAMs.

*Series 3, $F(CF_2)_x(CH_2)_ySH$.* Figure 2c shows the thicknesses of the Series 3 SAMs as a function of the number of perfluorinated carbon atoms. In this plot, the thicknesses show little variation throughout the entire series, reflecting the constant total chain length of 16 carbon atoms per adsorbate. Although the tilt angle of the perfluorocarbon segment increases when the length of the hydrocarbon segment is increased (which should plausibly influence film thickness), ellipsometry is unable to detect these predictably subtle differences in thickness.[58,81]

*Contact Angle Characterization. Series 1, $F(CF_2)_x(CH_2)_{11}SH$.* Figure 3a shows the wettabilities of pristine Series 1 SAMs determined

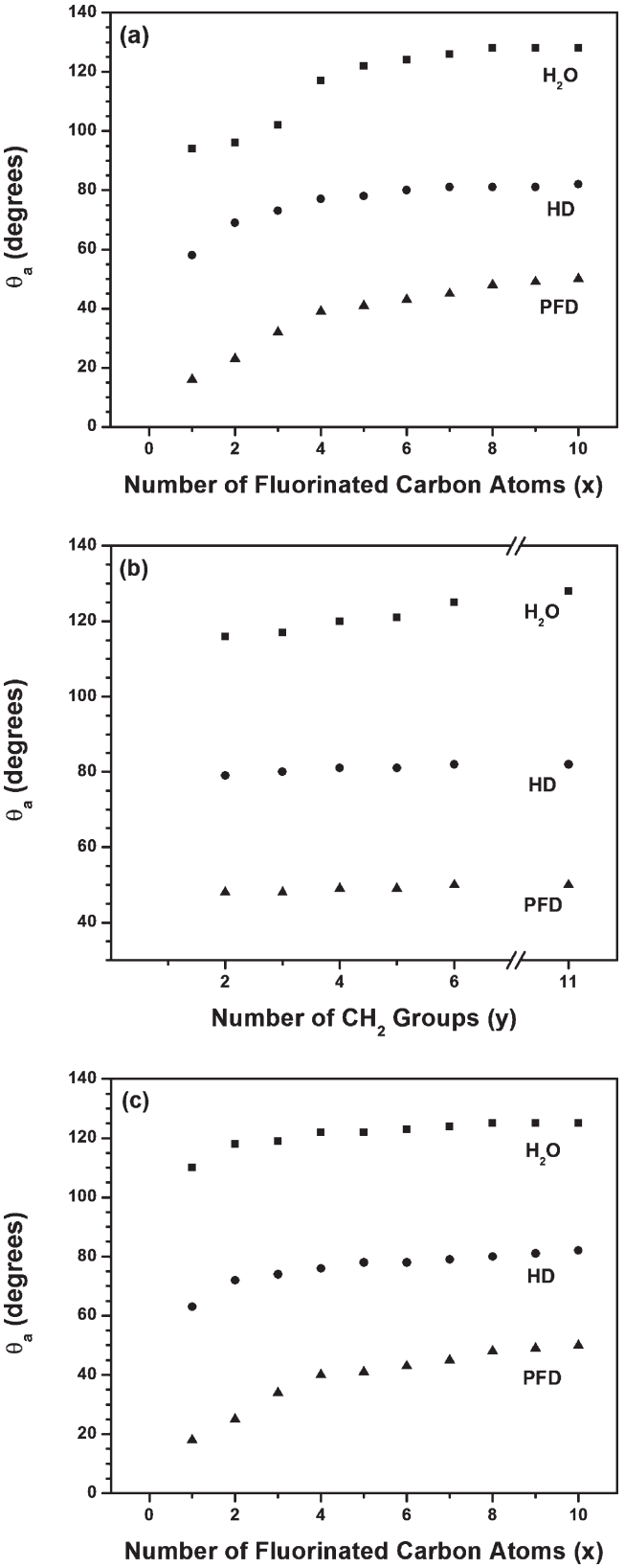


**Figure 3.** Advancing contact angles of water ($H_2O$), hexadecane (HD), and perfluorodecalin (PFD) on SAMs on gold generated from (a) Series 1, (b) Series 2, and (c) Series 3.

by advancing contact angle measurements ($\theta_a$) using water, HD, and PFD as contacting liquids. The advancing contact angles of water and HD suggest that these films become increasingly hydrophobic and oleophobic, respectively, as the number of perfluorinated carbon atoms ($x$) increases. The increase in advancing contact angle with increasing $x$ for all three liquids is consistent with a corresponding decrease in dispersive energy across the interface, which is plausibly due to a decrease in the surface density of $CF_3$ groups.[64] The enhanced increase in the advancing contact angles of water indicates that these films might be sensitive to the presence of fluorocarbon−hydrocarbon (FC−HC) dipoles.[64] As $x$ increases from 1 to 6, the contact angles increase due to decreased polar interactions between water and the surface of the SAMs. As $x$ increases, the FC−HC dipole is buried deeper into the film structure, increasing its distance from the polar contacting liquid, and thus decreasing the mutually attractive forces. At $x \geq 6$, the FC−HC dipole becomes sufficiently buried to the point that the dipoles are insensitive to the polar water molecules; consequently, the contact angles plateau to their maximum value.

*Series 2, $F(CF_2)_{10}(CH_2)_ySH$.* The molecular packing, structure, wettability, and thermal stability in air of SAMs generated from Series 2 maintaining a constant perfluorocarbon segment length while varying the methylene spacer have been previously described.[58,67] The advancing contact angles of pristine Series 2 SAMs when using water, HD, and PFD as contacting liquids are shown in Figure 3b. The average advancing contact angles of Series 2 SAMs for water ($\theta_a^{H_2O} = 120°$) and HD ($\theta_a^{HD} = 80°$) suggest both highly hydrophobic and oleophobic surfaces, respectively, consistent with films composed of high degrees of terminal perfluorination.[58] Large contact angles of HD arise from the characteristically weak dispersive interactions between fluorocarbons and hydrocarbons.[82] The small increase in the advancing contact angles of HD as the length of the methylene spacer ($y$) increases, where $y = 2$ ($\theta_a^{HD} = 78°$) and $y = 11$ ($\theta_a^{HD} = 82°$), might arise from a corresponding decrease in the distance-dependent van der Waals interactions between the contacting liquid and the underlying gold substrate.[83] We note, however, that no similar trend was observed when PFD was used as the contacting liquid; for PFD, the values remained nearly constant for all values of $y$.

Of the three contacting liquids, the advancing contact angles of water on Series 2 SAMs show the greatest increase in contact angle as the length of the methylene spacer ($y$) increases. As the number of $CH_2$ groups ($y$) increases from 2 to 11, the advancing contact angle of water increases from 116° to 128°, suggesting either that the interaction between the contacting liquid and the gold surface is not entirely dispersive in nature or that the water molecules intercalate more ready into the SAMs having shorter methylene spacers.[58,83]

*Series 3, $F(CF_2)_x(CH_2)_ySH$.* Figure 3c shows the wettabilities of the Series 3 SAMs using water, HD, and PFD as the contacting liquids. For each liquid, as the number of perfluorinated carbon atoms increases, there is an increase in the contact angle value. Although dipole interactions cannot be entirely excluded in the case of water,[82] the observed trend suggests that the dispersive interactions between the liquids and the SAMs decrease with increasing degree of fluorination, which is analogous to the trend observed for the Series 1 SAMs.[64,84]

**B. Thermal Desorption Studies.** Given that applications of organic thin films might require their use at elevated temperatures in solution environments, we compared the thermal desorption of the terminally perfluorinated SAMs in both a hydrocarbon (DC) and a perfluorocarbon (PFD) solvent. We chose these two solvents on the basis of the dual composition of

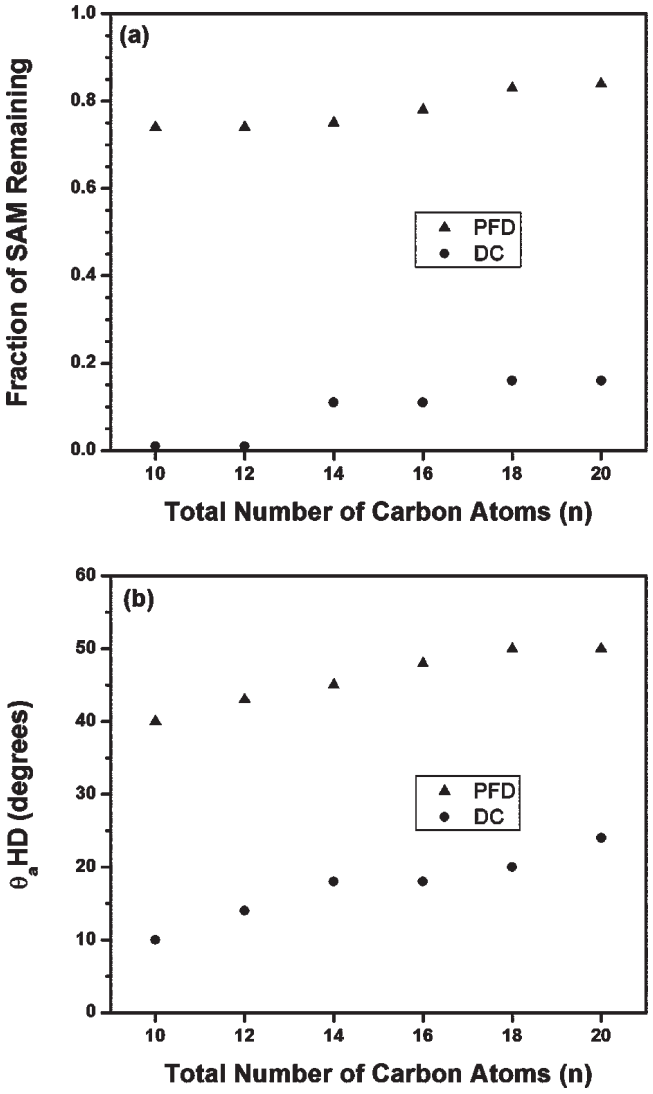


**Figure 4.** Heating of *n*-alkanethiol SAMs, $C_nSH$, in decalin (DC) and perfluorodecalin (PFD) at 80 °C for 90 min followed by the collection of (a) ellipsometric thicknesses and (b) advancing contact angles of hexadecane.

the SAMs and also on the fact that the bulkiness of these solvents versus their straight-chain counterparts might prevent their intercalation into the film assembly. In a previous study, we incubated SAMs on gold generated from terminally perfluorinated alkanethiols $F(CF_2)_{10}(CH_2)_xSH$, where $x$ = 2, 6, 11, 17, 33, in air for 1 h at various temperatures up to 180 °C.[58] The data showed that an increase in the length of the hydrocarbon segment stabilized the films against thermal degradation. This enhanced stability was attributed to a greater number of van der Waals interactions per adsorbate as the length of the hydrocarbon segment increased. Similarly, by maintaining a constant hydrocarbon segment length while varying the perfluorocarbon segment length, we observed an increase in thermal stability with increasing perfluorocarbon length. Interestingly, the thermal enhancement was greater per additional perfluoromethylene than per additional methylene.

In the present study, we used ellipsometry and contact angle measurements to monitor thermal desorption in solution to provide a more complete picture of both chain length and solvent effects on the stability of terminally perfluorinated SAMs on gold. To this end, we evaluated the thermal stabilities of SAMs generated from *n*-alkanethiols: $H(CH_2)_nSH$ ($C_nSH$), $F(CF_2)_x(CH_2)_{11}SH$ (Series 1), $F(CF_2)_{10}(CH_2)_ySH$ (Series 2), and $F(CF_2)_x(CH_2)_ySH$ (Series 3) by ex situ monitoring of their desorption into both a hydrocarbon (DC) and a perfluorocarbon (PFD) solvent. Desorption studies were performed by placing SAM-coated wafers into either DC or PFD held at 80 °C for 90 min. The extent of desorption was monitored by examining the changes in ellipsometric thickness[85] and the advancing contact angles of hexadecane.[86]

Ideally, our experiments would also include thermal desorption measurements of SAMs generated from semifluorinated adsorbates terminated by a hydrocarbon segment (e.g., $H(CH_2)_x(CF_2)_{11}SH$, $H(CH_2)_{10}(CF_2)_ySH$, and $H(CH_2)_x(CF_2)_ySH$) to provide greater insight into the factors that enhance the stability of semifluorinated films. Unfortunately, the synthesis of such adsorbates has proven to be considerably more difficult when compared with the synthesis of terminally perfluorinated adsorbates.

*SAMs from n-Alkanethiols, ($C_nSH$).* To provide a baseline reference, we first measured the thermal stability of SAMs on gold derived from *n*-alkanethiols, $C_nSH$, where $n$ = 10, 12, 14, 16, 18, 20, as a function of chain length under controlled conditions. Figure 4a and b shows the fraction of SAM remaining on the surface and the advancing contact angles of hexadecane (HD), respectively, upon thermal treatment. At first glance, two conclusions can be drawn from the data in Figure 4a: (1) the $C_nSH$ SAMs are significantly less stable in DC than in PFD and (2) the stability increases slightly in both solvents with increasing chain length. Because hexadecane contact angle measurements reflect the conformational order of hydrocarbon SAMs,[77−79] the advancing contact angle data in Figure 4b provide complementary support for the ellipsometric observations. Specifically, the advancing contact angles of $C_nSH$ SAMs heated in DC are ∼25−30° lower than the corresponding $C_nSH$ SAMs heated in PFD, indicating a considerably greater degree of surface disordering for the former SAMs. In addition, a similar enhancement in stability can be observed within the series as the chain length increases.

The enhanced desorption of $C_nSH$ SAMs in DC vs PFD might be due to (1) enhanced intercalation of the relatively small DC molecules into the film assemblies or (2) enhanced solvation of $C_nSH$ by DC (or both). In general, the thermal stability of the $C_nSH$ SAMs composed of longer methylene moieties display a greater resistance to film degradation upon heating in both solvents, which is consistent with the importance of interchain van der Waals interactions in film stabilization.[51]

*SAMs from Series 1, $F(CF_2)_x(CH_2)_{11}SH$.* We examined the influence of the length of the fluorocarbon segment on the thermal stability of terminally perfluorinated SAMs having a constant hydrocarbon spacer length. Figure 5a shows the thermal desorption data of Series 1 SAMs heated at 80 °C for 90 min in DC and PFD as a function of the length of the fluorocarbon segment ($x$). Although analysis of the data in Figure 5a indicates some degree of desorption upon heating in both solvents, it is readily apparent that the SAMs desorbed to a much greater extent in DC, particularly for those having short perfluorocarbon segments. As a representative example of the Series 1 SAMs, 46% of the SAM with $x$ = 7 desorbed upon heating in DC for 90 min compared with 12% desorption upon similar heating in PFD. Further, although 90% or more of the Series 1 SAMs having three

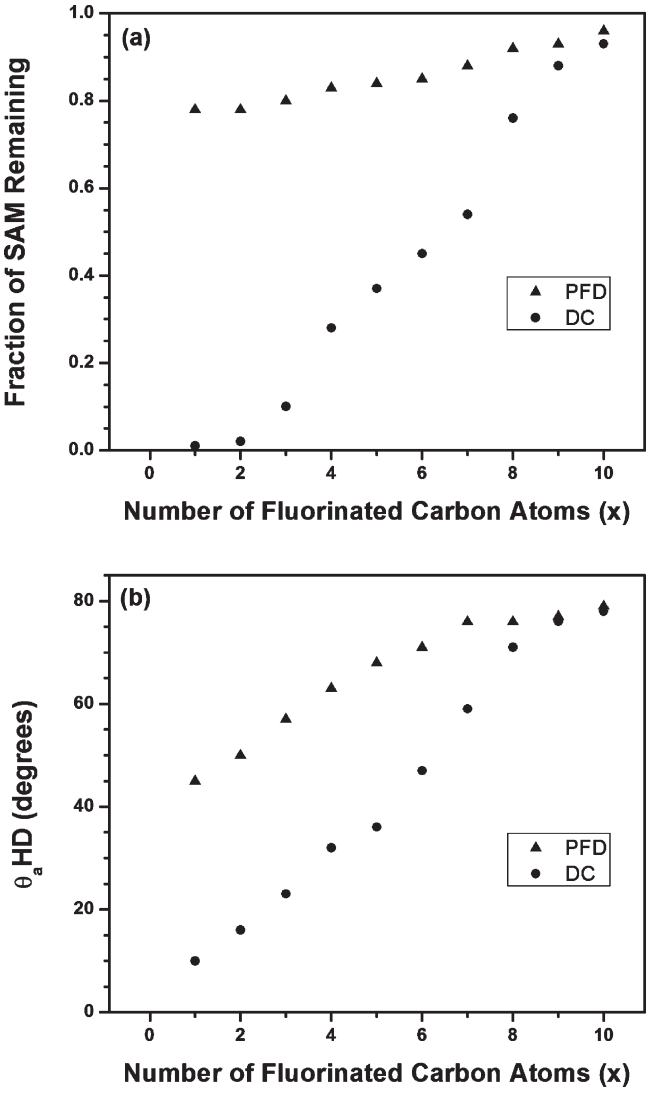


**Figure 5.** Heating of Series 1 SAMs, $F(CF_2)_x(CH_2)_{11}SH$, where $x$ = 1−10, in decalin (DC) and perfluorodecalin (PFD) at 80 °C for 90 min, followed by the collection of (a) ellipsometric thicknesses and (b) advancing contact angles of hexadecane.

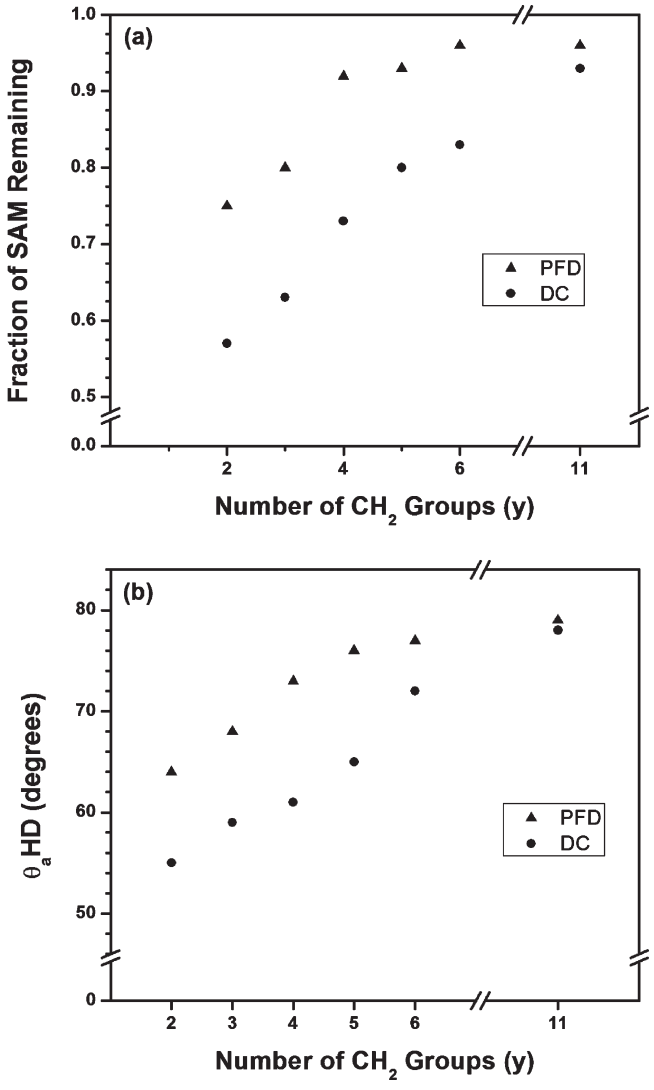


**Figure 6.** Heating of Series 2 SAMs, $F(CF_2)_{10}(CH_2)_ySH$, where $y$ = 2−6 and 11, in decalin (DC) and perfluorodecalin (PFD) at 80 °C for 90 min, followed by the collection of (a) ellipsometric thicknesses and (b) advancing contact angles of hexadecane.

or fewer perfluorinated carbon atoms desorbed upon heating in DC, those heated in PFD showed only modest desorption (<25%).

The thermal stabilities of the Series 1 SAMs were also assessed by monitoring changes in the advancing contact angles of HD. Figure 5b shows that the HD contact angles decreased systematically in DC and PFD as the length of the perfluorocarbon segment decreased, which is consistent with a decrease in order/packing. In addition, Figure 5b further supports the trend observed by ellipsometry in which desorption in DC is greater than that in PFD. Importantly, SAMs with $x \geq 8$ appeared to be quite robust in both DC and PFD at elevated temperatures.

*SAMs from Series 2, $F(CF_2)_{10}(CH_2)_ySH$.* With this series, we examined the influence of the length of the methylene spacer on the thermal stability of terminally perfluorinated SAMs having a constant fluorocarbon segment length. Analysis of the thermal desorption data in Figure 6a reveals that, again, the SAMs desorbed more readily in DC than in PFD. However, the differences between desorption in DC vs that in PFD were significantly reduced compared with those found with the Series 1 SAMs. Further, although Series 2 SAMs where $y$ = 11 showed substantial resistance to desorption in both DC and PFD, this resistance fell dramatically for $y \leq 6$, particularly for desorptions performed in DC. For example, where $y$ = 2, 75% of the SAM remained upon heating in PFD, but only 57% remained upon heating in DC.

The advancing contact angles of HD on Series 2 SAMs were also measured to evaluate the effects of thermal treatment. Figure 6b shows that upon heating in both solvents, the SAMs became more wettable with decreasing length of the methylene spacer; this trend was enhanced in DC compared with PFD. For example, we measured a $\theta_a^{HD}$ of 73° for $y$ = 6 and a $\theta_a^{HD}$ of 55° for $y$ = 2 after heating in DC. In contrast, we measured a $\theta_a^{HD}$ of 77° for $y$ = 6 and a $\theta_a^{HD}$ of 64° for $y$ = 2 after heating in PFD. These data indicate a loss of film order, a greater desorption in DC compared with PFD, or both. Furthermore, the thermal degradation of the SAMs in both solvents decreases with increasing length of the methylene spacer. Taken as a whole, however, the


dx.doi.org/10.1021/jp204970b |J. Phys. Chem. C 2011, 115, 19749–19760

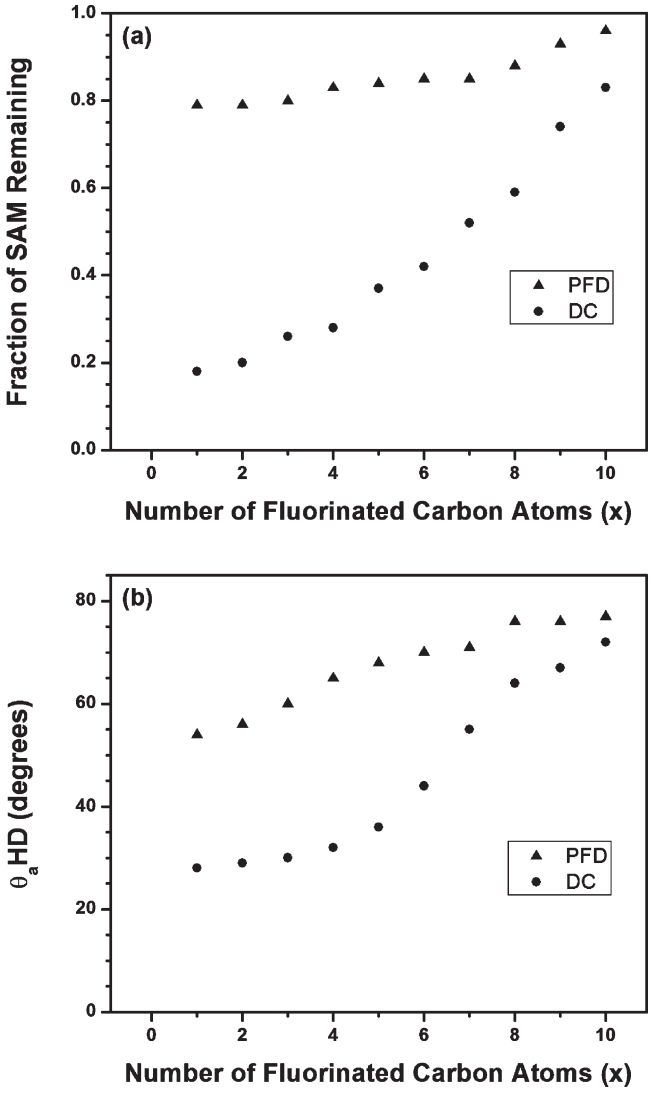


**Figure 7.** Heating of Series 3 SAMs, $F(CF_2)_x(CH_2)_ySH$, where $x$ = 1−10 and $y$ = 16 − $x$, in decalin (DC) and perfluorodecalin (PFD) at 80 °C for 90 min, followed by the collection of (a) ellipsometric thicknesses and (b) advancing contact angles of hexadecane.

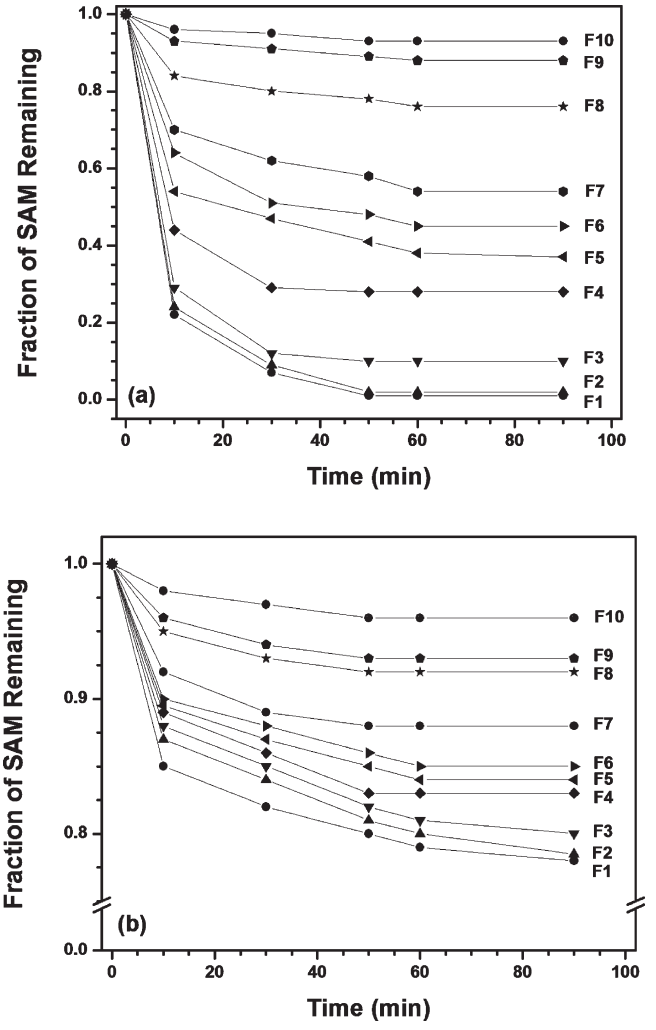


**Figure 8.** Fraction of Series 1 SAM remaining as a function of time after heating in (a) DC and (b) PFD at 80 °C.

data from both Series 1 and 2 support the conclusion that the thermal stability/degradation of terminally perfluorinated SAMs depends more strongly on the length of the fluorocarbon segment than on the length of the methylene spacer.[51]

*SAMs from Series 3, $F(CF_2)_x(CH_2)_ySH$.* In the two preceding series, we probed the effects of (1) varying the length of perfluorocarbon segment while holding the methylene spacer length constant and (2) varying the length of the methylene spacer while holding the perfluorocarbon segment length constant. To probe deeper, we generated SAMs from Series 3, in which both the length of the hydrocarbon and fluorocarbon segments were systematically varied while holding the total chain length constant at 16 carbon atoms. The data in Figure 7a show that the Series 3 SAMs are more resistant to desorption in PFD than in DC. Although the total chain length of these SAMs is constant, a clear distinction exists between the most highly fluorinated adsorbates (e.g., F10H6) and those having few perfluorinated carbon atoms (e.g., F1H15): the former are more resistant to desorption than the latter. In PFD, this difference is relatively small (4% desorption vs 22% desorption, respectively); in DC, however, the difference is markedly greater (6% desorption vs 98% desorption, respectively). On the basis of the general trend in both solvents that the more highly fluorinated SAMs are more resistant to desorption than those with less fluorination, we can conclude (as above) that the thermal stability/degradation of terminally perfluorinated SAMs is more strongly influenced by the length of the perfluorocarbon segment than the length of the methylene spacer.

We also measured the advancing contact angles of hexadecane on the thermally treated Series 3 SAMs. Figure 7b shows that there were systematic decreases in the value of $\theta_a^{HD}$ as a function of decreasing perfluorination; further, the decreases were amplified upon heating in DC vs PFD. These trends mirror the data from the ellipsometric measurements described in the preceding paragraph and thereby augment the conclusions presented therein.

*Desorption Kinetics of Terminally Perfluorinated SAMs on Gold.* For each of the SAMs, we examined the fraction of SAM remaining as a function of time upon heating at 80 °C in DC and PFD (Figures 8−9,10). All of the desorption profiles exhibit two common features: (1) a fast initial desorption regime followed by a slower or nondesorbing regime and (2) the fraction of SAM


dx.doi.org/10.1021/jp204970b |J. Phys. Chem. C 2011, 115, 19749–19760

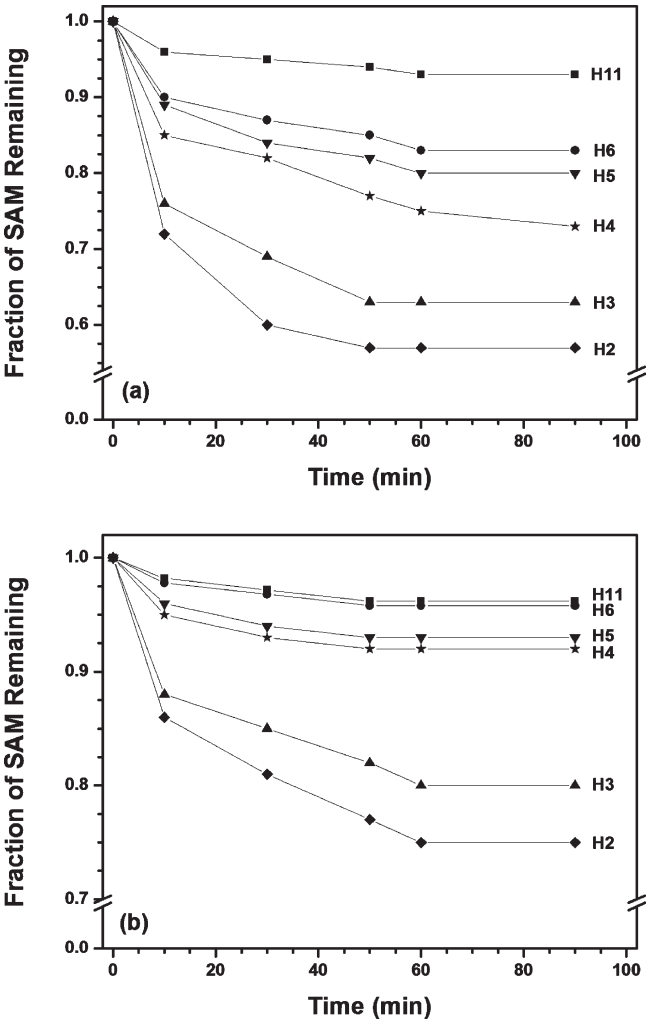


**Figure 9.** Fraction of Series 2 SAM remaining as a function of time after heating in (a) DC and (b) PFD at 80 °C.

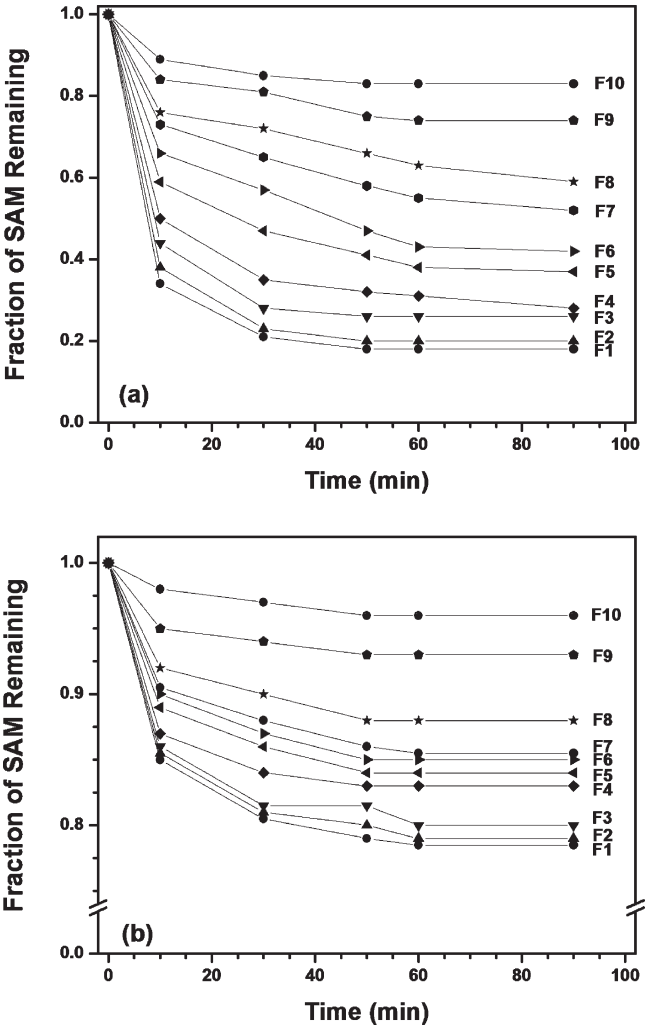


**Figure 10.** Fraction of Series 3 SAM remaining as a function of time after heating in (a) DC and (b) PFD at 80 °C.

remaining on the surface was greater at a given time for longer fluorocarbon and hydrocarbon segments. The presence of two distinct desorption regimes has been noted in previous studies of the desorption of SAMs on gold.[52,85,87] A two-site model of desorption was proposed to rationalize the observed two regimes.[85] Desorption of thiols from gold occurs rapidly at sites where thiols are weakly bound (site 1); little or no desorption occurs on sites where thiols are strongly bound (site 2). In the fast-desorbing regime (site 1), the structural features of the adsorbates might directly influence the rates of desorption. On the other hand, in the slow-desorbing regime, the thiols adsorbed to site 2 can either directly desorb from site 2 or diffuse to site 1 before desorbing from the surface, where the rate of diffusion of the thiolate species might also be strongly influenced by the structural features of the adsorbates.

To determine the relative rates of desorption for the adsorbates, we chose to examine the initial desorption profiles in the fast desorbing regime. In our analysis, we determined the initial rate constants ($k$) for desorption in the fast regime at 80 °C by means of first-order kinetics according to eq 1:

$$(T_t - T_\infty)/(T_0 - T_\infty) = e^{-kt} \quad (1)$$

**Table 1. First-Order Rate Constants for the Desorption of *n*-Alkanethiol SAMs ($C_nSH$) in the Fast-Desorbing Regime at 80 °C in Decalin (DC) and Perfluorodecalin (PFD)**

| $k \times 10^{-3}$ ($s^{-1}$) | $n = 10$ | 12 | 14 | 16 | 18 | 20 |
|---|---|---|---|---|---|---|
| $k$ (DC) | 3.0 | 3.0 | 2.9 | 2.7 | 2.4 | 2.3 |
| $k$ (PFD) | 2.4 | 2.4 | 2.3 | 2.2 | 2.4 | 2.3 |

where $T_0$ is the initial thickness of the SAM, $T_t$ is the thickness of the SAM at time $t$, and $T_\infty$ is the thickness of the slow/nondesorbing fraction of the SAM.[83]

Tables 1−4 give the initial rate constants for desorption in the fast desorbing regime in DC and PFD at 80 °C for SAMs derived from *n*-alkanethiols ($C_nSH$) and from each of the terminally perfluorinated akanethiols shown in Figure 1. The rate constants in Table 1 are consistent with those reported previously for the desorption in DC of SAMs on gold derived from *n*-alkanethiols ($C_nSH$).[52] As a whole, the rate constants for the $C_nSH$ SAMs are larger in DC than in PFD; moreover, they decrease as the length of the hydrocarbon chain increases in DC, but are relatively constant for all chain lengths in PFD. When the hydrocarbon chain becomes sufficiently long ($n \geq 18$), the rate constants in

**Table 2. First-Order Rate Constants for the Desorption of Series 1 SAMs ($F_xH_{11}SH$) in the Fast-Desorbing Regime at 80 °C in Decalin (DC) and Perfluorodecalin (PFD)**

| $k \times 10^{-3}$ ($s^{-1}$) | $x = 1$ | 2 | 3 | 4 | 5 | 6 | 7 | 8 | 9 | 10 |
|---|---|---|---|---|---|---|---|---|---|---|
| $k$ (DC) | 2.5 | 2.4 | 2.6 | 2.5 | 2.2 | 1.8 | 1.8 | 1.8 | 1.5 | 1.4 |
| $k$ (PFD) | 1.9 | 1.5 | 1.5 | 1.7 | 1.9 | 1.8 | 1.8 | 1.6 | 1.4 | 1.2 |

**Table 3. First-Order Rate Constants for the Desorption of Series 2 SAMs ($F_{10}H_ySH$) in the Fast-Desorbing Regime at 80 °C in Decalin (DC) and Perfluorodecalin (PFD)**

| $k \times 10^{-3}$ ($s^{-1}$) | $y = 2$ | 3 | 4 | 5 | 6 | 11 |
|---|---|---|---|---|---|---|
| $k$ (DC) | 1.8 | 1.7 | 1.4 | 1.3 | 1.5 | 1.4 |
| $k$ (PFD) | 1.4 | 1.5 | 1.6 | 1.4 | 1.2 | 1.1 |

**Table 4. First-Order Rate Constants for the Desorption of Series 3 SAMs ($F_xH_{16-x}SH$) in the Fast-Desorbing Regime at 80 °C in Decalin (DC) and Perfluorodecalin (PFD)**

| $k \times 10^{-3}$ ($s^{-1}$) | $x = 1$ | 2 | 3 | 4 | 5 | 6 | 7 | 8 | 9 | 10 |
|---|---|---|---|---|---|---|---|---|---|---|
| $k$ (DC) | 2.7 | 2.5 | 2.4 | 2.0 | 1.8 | 1.5 | 1.4 | 1.5 | 1.6 | 1.6 |
| $k$ (PFD) | 2.0 | 2.0 | 2.0 | 2.1 | 1.9 | 1.9 | 1.8 | 1.8 | 1.8 | 1.2 |

DC begin to match those in PFD, suggesting that the rate-determining step for desorption becomes the same at long chain lengths for the two solvent systems.

For the Series 1 SAMs (Table 2 and Figure 8), the initial rate constants generally decrease as the length of the perfluorocarbon segment increases in both DC and PFD. Moreover, the SAMs desorb more readily in DC than in PFD, particularly for the adsorbates having short perfluorocarbon segments. The kinetics data from the Series 2 SAMs (Table 3 and Figure 9) can be interpreted to indicate that the stability afforded to the terminally perfluorinated SAMs derives largely from the long perfluorocarbon segment (F10) with only a minimal increase in stability afforded by lengthening the methylene spacer. When examining the absolute difference in the rate constants from the shortest ($y = 2$) to the longest ($y = 11$) methylene segment in both DC and PFD, only small differences exist compared with those derived from the Series 1 SAMs, for which the differences are considerably larger for the shortest ($x = 2$) vs the longest ($x = 10$) perfluorocarbon segment.

The desorption kinetics for the Series 3 SAMs are shown in Table 4 and Figure 10. The initial rates of desorption decrease in DC (and perhaps PFD) as the length of the perfluorocarbon segment increases and the length of the methylene spacer decreases. Furthermore, the rates of desorption in DC vs those in PFD appear to follow no obvious trend.

To determine whether desorbed molecules in solution influence the desorption kinetics of the monolayers, we examined the fraction of a $C_{18}SH$ SAM remaining as a function of time upon consecutively immersing the monolayer in three fresh portions of DC at 80 °C (Figure 11). The monolayer was immersed into fresh portions of DC at the beginning, 10 min after heating, and 30 min after heating. The thickness of the monolayer was monitored and compared with another $C_{18}SH$ SAM that was immersed in only one portion of DC at 80 °C. As shown in Figure 11, the two desorption profiles are almost identical, indicating that desorbed molecules have no influence on the desorption kinetics.

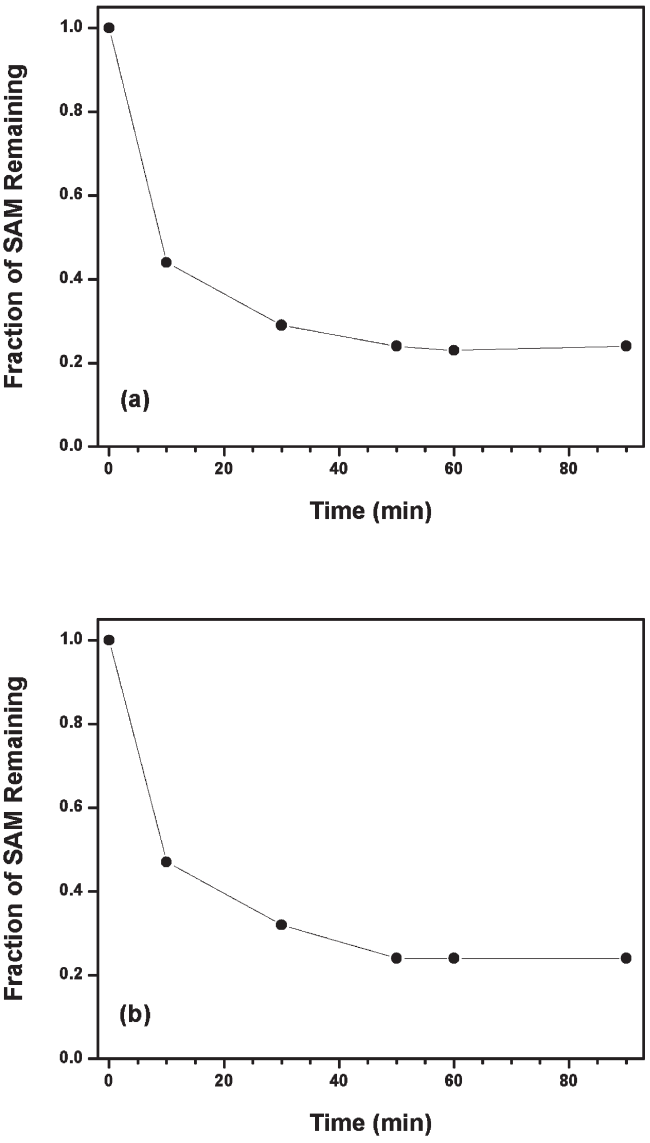


**Figure 11.** Fraction of $C_{18}SH$ SAM remaining as a function of time after heating at 80 °C in (a) DC and in (b) fresh portions of DC at $t = 0$, 10, and 30 min.

When broadly considering the results obtained from our thermal desorption experiments, we can conclude that the thermal stability of Series 1 SAMs increases with increasing length of the perfluorocarbon chain when heated in contact with both DC and PFD. Moreover, the fastest desorption and greatest loss of packing/order occurred with adsorbates composed of shorter perfluorocarbon segments in DC. Overall, long perfluorocarbon segments give rise to enhanced stability in both DC and PFD at elevated temperature.

On the whole, the Series 2 SAMs exhibited greater resistance to thermal desorption in both DC and PFD than did the Series 1 SAMs. This trend reflects the greater stabilizing ability, with regard to thermal desorption, of incorporating high degrees of terminal perfluorination into film assemblies. Collectively, the data further suggest that the Series 2 SAMs are less thermally stable in DC than in PFD, perhaps due to ready penetration of the smaller and less oleophobic DC molecules into the film assembly.

With the Series 3 SAMs, we chose to maintain a constant carbon chain length and vary the length of the perfluorocarbon and hydrocarbon segments dependently. In this system, we wished to determine which portion of the fluorinated film (hydrocarbon vs fluorocarbon) imparted greater stability toward thermal desorption. An increase in fluorocarbon length meant a consequent decrease in the methylene spacer, allowing for direct observation of stability effects based on either the perfluorocarbon or hydrocarbon segment. In general, the thermal stability showed greater dependence on the length of the perfluorocarbon segment, although the SAMs having longer methylene segments also exhibited enhanced stability. Further, SAMs exposed to heated solutions of PFD displayed increased resistance to desorption compared with those heated in DC.

As a whole, the experiments reported here reveal two significant trends. First, all of the SAMs desorb more readily in DC than in PFD. Second, the length of the perfluorocarbon segment has a greater impact on stability than the length of the hydrocarbon segment. The first trend can perhaps be rationalized by solvent intercalation. We note that PFD is substantially larger than DC by ∼54%, on the basis of their relative molar volumes; this calculation is based on the estimated relative molar volumes of PFD, 237.5 mL/mol, and DC, 154.2 mL/mol.[88] In this regard, DC molecules can conceivably intercalate more readily than PFD into the films at elevated temperatures, solubilizing their tail groups and enhancing their desorption. If this interpretation is valid, then the intercalation effect for the perfluorinated films at elevated temperatures must be sufficient to overcome the well-known poor solubility of perfluorocarbons in hydrocarbon solvents.[89]

Regarding the second trend, the enhanced stability afforded predominantly by the perfluorocarbon segment can be rationalized on the basis of stronger solid-state fluorocarbon−fluorocarbon interactions than hydrocarbon−hydrocarbon interactions.[90] Given that the terminally fluorinated SAMs and the hydrocarbon SAMs reported here are all crystalline in nature,[69,81,91−100] their solid-state thermal stability can be evaluated with respect to the melting points of *n*-perfluoroalkanes, semifluorinated *n*-alkanes ($F(CF_2)_x(CH_2)_y$-H), and *n*-alkanes.[90,101−104] It is known that *n*-perfluoroalkanes melt at higher temperatures than the corresponding semifluorinated *n*-alkanes, $F(CF_2)_x(CH_2)_yH$, which melt at higher temperatures than the corresponding *n*-alkanes.[90] Given these data and assuming that the initial steps of the thermal degradation of SAMs can be viewed as a "melting" of the crystalline chains to form liquidlike films, SAMs with a longer perfluorocarbon moiety would be expected to "melt" or disorder at a higher temperature than SAMs with a shorter perfluorocarbon moiety. Although the correlation between this type of "melting" transition and film degradation is complicated by uncertainties involving the products and mechanism of the decomposition of SAMs on gold,[29,77,105] it might be plausible to view the "melting" transition as a prelude to film degradation.

In addition, given that perfluorocarbon segments have a helical van der Waals diameter of 5.8 Å and hydrocarbon segments have a trans-extended van der Waals diameter of 4.2 Å,[65,67] one might assume that the hydrocarbon segments in semifluorinated SAMs experience reduced van der Waals interactions due to the greater separation of the chains as a result of the bulkier terminal fluorocarbon segment. However, previous studies have found that the $CH_2$ moieties in these terminally perfluorinated SAMs are more tilted from the surface normal than those in *n*-alkanethiol SAMs.[69] Consequently, although it is true that the sulfur headgroups are further apart in F-SAMs than in H-SAMs, the $CH_2$ groups in both types of SAMs maintain intimate van der Waals contact. Overall, these studies indicate that the thermal stability of terminally perfluorinated SAMs on gold can be enhanced by increasing the lengths of the hydrocarbon, particularly the perfluorocarbon segments.

## CONCLUSIONS

We generated SAMs on gold from three series of terminally perfluorinated alkanethiols; (1) Series 1, $F(CF_2)_x(CH_2)_{11}SH$, where $x = 1−10$; (2) Series 2, $F(CF_2)_{10}(CH_2)_ySH$, where $y = 2−6, 11$; and (3) Series 3, $F(CF_2)_x(CH_2)_ySH$ where $x = 1−10$ and $y = 16 − x$. The resulting films were characterized using ellipsometry and contact angle goniometry to measure initial film thicknesses and advancing contact angles. Measured ellipsometric thicknesses from Series 1, 2, and 3 SAMs indicate the formation of films composed of single layer thicknesses. Initial average advancing contact angles of water ($\theta_a$ = ∼120°; $H_2O$) and hexadecane ($\theta_a$ = ∼80°; HD) further suggest that all three series of PFA SAMs are highly hydrophobic and oleophobic, respectively, consistent with a surface primarily composed of densely packed $CF_3$-terminated groups.[92] SAMs derived from *n*-alkanethiols ($C_nSH$) were also prepared as baseline standards to evaluate the thermal stability of the terminally perfluorinated SAMs. The results presented here suggest that both terminally perfluorinated and hydrocarbon SAMs are less thermally stable in DC than in PFD, perhaps due to ready penetration of the smaller DC molecules into the film assembly. Moreover, the stabilities of terminally perfluorinated SAMs can be enhanced by increasing either the length of the $CF_2$ or $CH_2$ segments, with the most influential parameter being the length of the $CF_2$ segments.

## AUTHOR INFORMATION

### Corresponding Author

*E-mail: henry.moore@utb.edu (H.J.M.); trlee@uh.edu (T.R.L.).

## ACKNOWLEDGMENT

We are grateful for support from Seiko Epson Corporation, the National Science Foundation (DMR-0906727), the Robert A. Welch Foundation (Grant No. E-1320), and the Texas Center for Superconductivity at the University of Houston. Support for work at the University of Texas at Brownsville was generously provided by a Departmental Grant from the Robert A. Welch Foundation (Grant No. BQ-0038).

## REFERENCES

(1) Bigelow, W. C.; Pickett, D. L.; Zisman, W. A. *J. Colloid Sci.* **1946**, *1*, 513–538.

(2) Taniguchi, I.; Toyosawa, K.; Yamaguchi, H.; Yasukouchi, K. *Chem. Commun.* **1982**, *18*, 1032–1033.

(3) Nuzzo, R. G.; Allara, D. L. *J. Am. Chem. Soc.* **1983**, *105*, 4481–4483.

(4) Halik, M.; Klauk, H.; Zschieschang, U.; Schmid, G.; Dehm, C.; Schutz, M.; Maisch, S.; Effenberger, F.; Brunnbauer, M.; Stellacci, F. *Nature* **2004**, *431*, 963–966.

(5) Tai, Y.; Shaporenko, A.; Noda, H.; Grunze, M.; Zharnikov, M. *Adv. Mater.* **2005**, *17*, 1745–1749.

(6) Hamadani, B. H.; Corley, D. A.; Ciszek, J. W.; Tour, J. M.; Natelson, D. *Nano Lett.* **2006**, *6*, 1303–1306.

(7) Holzl, M.; Tinazli, A.; Leitner, C.; Hahn, C. D.; Lackner, B.; Tampe, R.; Gruber, H. J. *Langmuir* **2007**, *23*, 5571–5577.
(8) Kankate, L.; Werner, U.; Turchanin, A.; Gölzhäuser, A.; Großmann, H.; Tampé, R. *Biointerphases* **2010**, *5*, 30–36.
(9) Béthencourt, M. I.; Barriet, D.; Frangi, N. M.; Lee, T. R. *J. Adhes.* **2005**, *81*, 1031–1048.
(10) Mueller, W.; Ringsdorf, H.; Rump, E.; Wildburg, G.; Zhang, X.; Angermaier, L.; Knoll, W.; Liley, W.; Spinke, J. *Science* **1993**, *262*, 1706–1708.
(11) Haeussling, L.; Ringsdorf, H.; Schmitt, F. J.; Knoll, W. *Langmuir* **1991**, *7*, 1837–1840.
(12) Limbut, W.; Kanatharana, P.; Mattiasson, B.; Asawatreratanakul, P.; Thavarungkul, P. *Biosens. Bioelectron.* **2006**, *22*, 233–240.
(13) Disley, D. M.; Morrill, P. R.; Sproule, K.; Lowe, C. R. *Biosens. Bioelectron.* **1999**, *14*, 481–493.
(14) Moccelini, S. K.; Vieira, I. C.; de Lima, F.; Lucca, B. G.; Barbosa, A. M. J.; Ferreira, V. S. *Talanta* **2010**, *82*, 164–170.
(15) Kincaid, H. A.; Niedringhaus, T.; Ciobanu, M.; Cliffel, D. E.; Jennings, G. K. *Langmuir* **2006**, *22*, 8114–8120.
(16) Kim, M.; Hohman, J. N.; Cao, Y.; Houk, K. N.; Ma, H.; Jen, A. K.-Y.; Weiss, P. S. *Science* **2011**, *331*, 1312–1315.
(17) Jennings, G. K.; Laibinis, P. E. *Colloids Surf, A* **1996**, *116*, 105–114.
(18) Jennings, G. K.; Munro, J. C.; Laibinis, P. E. *Adv. Mater.* **1999**, *11*, 1000–1003.
(19) Jennings, G. K.; Munro, J. C.; Yong, T. H.; Laibinis, P. E. *Langmuir* **1998**, *14*, 6130–6139.
(20) Jennings, G. K.; Yong, T. H.; Munro, J. C.; Laibinis, P. E. *J. Am. Chem. Soc.* **2003**, *125*, 2950–2957.
(21) Whelan, C. M.; Kinsella, M.; Carbonell, L.; Meng, Ho, H.; Maex, K. *Microelectron. Eng.* **2003**, *70*, 551–557.
(22) Zamborini, F. P.; Crooks, R. M. *Langmuir* **1998**, *14*, 3279–3286.
(23) Ishizaki, T.; Okido, M.; Masuda, Y.; Saito, N.; Sakamoto, M. *Langmuir* **2011**, *27*, 6009–6017.
(24) Porter, M. D.; Bright, T. B.; Allara, D. L.; Chidsey, C. E. D. *J. Am. Chem. Soc.* **1987**, *109*, 3559–3568.
(25) Bain, C. D.; Troughton, E. B.; Tao, Y. T.; Evall, J.; Whitesides, G. M.; Nuzzo, R. G. *J. Am. Chem. Soc.* **1989**, *111*, 321–335.
(26) Willey, T. M.; Vance, A. L.; van Buuren, T.; Bostedt, C.; Terminello, L. J.; Fadley, C. S. *Surf. Sci.* **2005**, *576*, 188–196.
(27) Kumar, A.; Biebuyck, H. A.; Whitesides, G. M. *Langmuir* **1994**, *10*, 1498–1511.
(28) Laibinis, P. E.; Whitesides, G. M. *J. Am. Chem. Soc.* **1992**, *114*, 9022–9028.
(29) Bensebaa, F.; Ellis, T. H.; Badia, A.; Lennox, R. B. *Langmuir* **1998**, *14*, 2361–2367.
(30) Norrod, K. L.; Rowlen, K. L. *J. Am. Chem. Soc.* **1998**, *120*, 2656–2657.
(31) Schoenfisch, M. H.; Pemberton, J. E. *J. Am. Chem. Soc.* **1998**, *120*, 4502–4513.
(32) Zhang, Y.; Terrill, R. H.; Tanzer, T. A.; Bohn, P. W. *J. Am. Chem. Soc.* **1998**, *120*, 2654–2655.
(33) Li, Y.; Huang, J.; McIver, R. T., Jr.; Hemminger, J. C. *J. Am. Chem. Soc.* **1992**, *114*, 2428–2432.
(34) Heister, K.; Allara, D. L.; Bahnck, K.; Frey, S.; Zharnikov, M.; Grunze, M. *Langmuir* **1999**, *15*, 5440–5443.
(35) Kakiuchi, T.; Sato, K.; Iida, M.; Hobara, D.; Imabayashi, S.; Niki, K. *Langmuir* **2000**, *16*, 7238–7244.
(36) Schlenoff, J. B.; Li, M.; Ly, H. *J. Am. Chem. Soc.* **1995**, *117*, 12528–12536.
(37) Imabayashi, S.; Hobara, D.; Kakiuchi, T. *Langmuir* **2001**, *17*, 2560–2563.
(38) Schonherr, H.; Ringsdorf, H.; Jaschke, M.; Butt, H. J.; Bamberg, E.; Allinson, H.; Evans, S. D. *Langmuir* **1996**, *12*, 3898–3904.
(39) Tam-Chang, S.-W.; Biebuyck, H. A.; Whitesides, G. M.; Jeon, N.; Nuzzo, R. G. *Langmuir* **1995**, *11*, 4371–4382.
(40) Clegg, R. S.; Reed, S. M.; Hutchison, J. E. *J. Am. Chem. Soc.* **1998**, *120*, 2486–2487.
(41) Valiokas, R.; Ostblom, M.; Svedhem, S.; Svensson, S. C. T.; Liedberg, B. *J. Phys. Chem. B* **2002**, *106*, 10401–10409.
(42) Lewis, P. A.; Smith, R. K.; Kelly, K. F.; Bumm, L. A.; Reed, S. M.; Clegg, R. S.; Gunderson, J. D.; Hutchison, J. E.; Weiss, P. S. *J. Phys. Chem. B* **2001**, *105*, 10630–10636.
(43) Garg, N.; Friedman, J. M.; Lee, T. R. *Langmuir* **2000**, *16*, 4266–4271.
(44) Garg, N.; Lee, T. R. *Langmuir* **1998**, *14*, 3815–3819.
(45) Park, B.; Lorenz, C. D.; Chandross, M.; Stevens, M. J.; Grest, G. S.; Borodin, O. A. *Langmuir* **2004**, *20*, 10007–10014.
(46) Park, J. S.; Smith, A. C.; Lee, T. R. *Langmuir* **2004**, *20*, 5829–5836.
(47) Park, J. S.; Vo, A. N.; Barriet, D.; Shon, Y. S.; Lee, T. R. *Langmuir* **2005**, *21*, 2902–2911.
(48) Shon, Y. S.; Colorado, R.; Williams, C. T.; Bain, C. D.; Lee, T. R. *Langmuir* **2000**, *16*, 541–548.
(49) Shon, Y. S.; Lee, S.; Colorado, R.; Perry, S. S.; Lee, T. R. *J. Am. Chem. Soc.* **2000**, *122*, 7556–7563.
(50) Shon, Y. S.; Lee, S.; Perry, S. S.; Lee, T. R. *J. Am. Chem. Soc.* **2000**, *122*, 1278–1281.
(51) Shon, Y. S.; Lee, T. R. *J. Phys. Chem. B* **2000**, *104*, 8182–8191.
(52) Shon, Y. S.; Lee, T. R. *J. Phys. Chem. B* **2000**, *104*, 8192–8200.
(53) Wooster, T. T.; Gamm, P. R.; Geiger, W. E.; Oliver, A. M.; Black, A. J.; Craig, D. C.; Paddon-Row, M. N. *Langmuir* **1996**, *12*, 6616–6626.
(54) Turchanin, A.; El-Desawy, M.; Gölzhäuser, A. *Appl. Phys. Lett.* **2007**, *90*, 053102.
(55) Jennings, G. K.; Laibinis, P. E. *Langmuir* **1996**, *12*, 6173–6175.
(56) Lin, S. Y.; Tsai, T. K.; Lin, C. M.; Chen, C. h.; Chan, Y. C.; Chen, H. W. *Langmuir* **2002**, *18*, 5473–5478.
(57) Chen, C. C.; Chen, I. W. P.; Lin, S. Y.; Chen, C. h. *J. Phys. Chem. B* **2004**, *108*, 17497–17504.
(58) Fukushima, H.; Seki, S.; Nishikawa, T.; Takiguchi, H.; Tamada, K.; Abe, K.; Colorado, R.; Graupe, M.; Shmakova, O. E.; Lee, T. R. *J. Phys. Chem. B* **2000**, *104*, 7417–7423.
(59) Kondoh, H.; Kodama, C.; Sumida, H.; Nozoye, H. *J. Chem. Phys.* **1999**, *111*, 1175–1184.
(60) Dubois, L. H.; Zegarski, B. R.; Nuzzo, R. G. *Langmuir* **1986**, *2*, 412–417.
(61) Alves, C. A.; Porter, M. D. *Langmuir* **1993**, *9*, 3507–3512.
(62) Chidsey, C. E. D.; Loiacono, D. N. *Langmuir* **1990**, *6*, 682–691.
(63) Colorado, R.; Lee, T. R. *J. Phys. Chem. B* **2003**, *107*, 10216–10220.
(64) Colorado, R.; Lee, T. R. *Langmuir* **2003**, *19*, 3288–3296.
(65) Liu, G. Y.; Fenter, P.; Chidsey, C. E. D.; Ogletree, D. F.; Eisenberger, P.; Salmeron, M. *J. Chem. Phys.* **1994**, *101*, 4301–4306.
(66) Schonherr, H.; Vancso, G. J. *Langmuir* **1997**, *13*, 3769–3774.
(67) Tamada, K.; Ishida, T.; Knoll, W.; Fukushima, H.; Colorado, R.; Graupe, M.; Shmakova, O. E.; Lee, T. R. *Langmuir* **2001**, *17*, 1913–1921.
(68) Tsao, M. W.; Hoffmann, C. L.; Rabolt, J. F.; Johnson, H. E.; Castner, D. G.; Erdelen, C.; Ringsdorf, H. *Langmuir* **1997**, *13*, 4317–4322.
(69) Frey, S.; Heister, K.; Zharnikov, M.; Grunze, M.; Tamada, K.; Colorado, R.; Graupe, M.; Shmakova, O. E.; Lee, T. R. *Isr. J. Chem.* **2000**, *40*, 81–97.
(70) Weinstein, R. D.; Moriarty, J.; Cushnie, E.; Colorado, R.; Lee, T. R.; Patel, M.; Alesi, W. R.; Jennings, G. K. *J. Phys. Chem. B* **2003**, *107*, 11626–11632.
(71) Wagner, A. J.; Wolfe, G. M.; Fairbrother, D. H. *J. Chem. Phys.* **2004**, *120*, 3799–3810.
(72) Garbassi, F.; Morroca, M.; Occhiello, E. *Polymer Surfaces.* Wiley: Chichester, U.K., 1994.
(73) Kinloch, A. J. *Adhesion and Adhesives*; Chapman and Hall: New York, 1987.
(74) Wu, S. *Polymer Interface and Adhesion*; Marcel Decker: New York, 1982.
(75) Graupe, M.; Koini, T.; Wang, V. Y.; Nassif, G. M.; Colorado, R.; Villazana, R. J.; Dong, H.; Miura, Y. F.; Shmakova, O. E.; Lee, T. R. *J. Fluorine Chem.* **1999**, *93*, 107–115.

(76) Sellers, H.; Ulman, A.; Shnidman, Y.; Eilers, J. E. *J. Am. Chem. Soc.* **1993**, *115*, 9389.
(77) Ulman, A. *An Introduction to Ultrathin Organic Thin Films*; Academic Press: Boston, 1991.
(78) Tao, Y. T. *J. Am. Chem. Soc.* **1993**, *115*, 4350–4358.
(79) Berg, J. C. *Wettability*: Marcel Decker: New York, 1993.
(80) Colorado, R., Jr.; Graupe, M.; Shmakova, O. E.; Villazana, R. J.; Lee, T. R. In *Interfacial Properties on the Submicron Scale*; Frommer, J. E., Overney, R., Eds.; ACS Symposium Series 781; American Chemical Society: Washington, DC, 2001; pp 276−292.
(81) Tamada, K.; Nagasawa, J.; Nakanishi, F.; Abe, K.; Hara, M.; Knoll, W.; Ishida, T.; Fukushima, H.; Miyashita, S.; Usui, T.; Koini, T.; Lee, T. R. *Thin Solid Films* **1998**, *329*, 150–155.
(82) Chaudhury, M. K. *Mater. Sci. Eng., R Rep.* **1996**, *16*, 97–159.
(83) Miller, W. J.; Abbott, N. L. *Langmuir* **1997**, *13*, 7106–7114.
(84) Colorado, R.; Lee, T. R. *J. Phys. Org. Chem.* **2000**, *13*, 796–807.
(85) Garg, N.; Carrasquillo-Molina, E.; Lee, T. R. *Langmuir* **2002**, *18*, 2717–2726.
(86) Lee, T. C.; Hounihan, D. J.; Colorado, R.; Park, J. S.; Lee, T. R. *J. Phys. Chem. B* **2004**, *108*, 2648–2653.
(87) Walczak, M. M.; Alves, C. A.; Lamp, B. D.; Porter, M. D. *J. Electroanal. Chem.* **1995**, *396*, 103–114.
(88) Budavari, S. *The Merck Index*, 11th ed.; Merck & Co., Inc.: Rahway, NJ, USA, 1989, pp 447−448 and 655.
(89) Broniatowski, M.; VilaRomeu, N.; Dynarowicz-Latka, P. *J. Phys. Chem. B* **2006**, *110*, 3078–3087.
(90) Rabolt, J. F.; Russell, T. P.; Twieg, R. J. *Macromolecules* **1984**, *17*, 2786–2794.
(91) Kim, H. I.; Koini, T.; Lee, T. R.; Perry, S. S. *Langmuir* **1997**, *13*, 7192–7196.
(92) Kim, H. I.; Koini, T.; Lee, T. R.; Perry, S. S. *Tribol. Lett.* **1998**, *4*, 137–140.
(93) Miura, Y. F.; Takenaga, M.; Koini, T.; Graupe, M.; Garg, N.; Graham, R. L.; Lee, T. R. *Langmuir* **1998**, *14*, 5821–5825.
(94) Graupe, M.; Koini, T.; Kim, H. I.; Garg, N.; Miura, Y. F.; Takenaga, M.; Perry, S. S.; Lee, T. R. *MRS Bull.* **1999**, *34*, 447–453.
(95) Graupe, M.; Koini, T.; Kim, H. I.; Garg, N.; Miura, Y. F.; Takenaga, M.; Perry, S. S.; Lee, T. R. *Colloids Surf., A* **1999**, *154*, 239–244.
(96) Kim, H. I.; Graupe, M.; Oloba, O.; Koini, T.; Imaduddin, S.; Lee, T. R.; Perry, S. S. *Langmuir* **1999**, *15*, 3179–3185.
(97) Colorado, R., Jr.; Graupe, M.; Takenaga, M.; Koini, T.; Lee, T. R. *Mater. Res. Soc. Symp. Proc.* **1999**, *546*, 237–242.
(98) Graupe, M.; Takenaga, M.; Koini, T.; Colorado, R., Jr.; Lee, T. R. *J. Am. Chem. Soc.* **1999**, *121*, 3222–3223.
(99) Frey, S.; Heister, K.; Zharnikov, M.; Grunze, M.; Colorado, R., Jr.; Graupe, M.; Shmakova, O. E.; Lee, T. R. *Phys. Chem. Chem. Phys.* **2000**, *2*, 1979–1987.
(100) Colorado, R., Jr.; Graupe, M.; Kim, H. I.; Takenaga, M.; Oloba, O.; Lee, S.; Perry, S. S.; Lee, T. R. In *Interfacial Properties on the Submicron Scale*; Frommer, J. E., Overney, R., Eds.; ACS Symposium Series 781; American Chemical Society: Washington, DC, 2001; pp 58−75.
(101) Scott, R. L. *J. Am. Chem. Soc.* **1948**, *70*, 4090–4093.
(102) Russell, T. P.; Rabolt, J. F.; Twieg, R. J.; Siemens, R. L.; Farmer, B. L. *Macromolecules* **1986**, *19*, 1135–1142.
(103) Broniatowski, M.; Dynarowicz-Łątka, P.; Witko, W. *J. Fluorine Chem.* **2005**, *126*, 79–86.
(104) Broniatowski, M.; Dynarowicz-Łątka, P. *Adv. Colloid Interface Sci.* **2008**, *138*, 63–83.
(105) Evans, S. D.; Urankar, E.; Ulman, A.; Ferris, N. *J. Am. Chem. Soc.* **1991**, *113*, 4121–4131.